British Journal of Nutrition (2022), 127, 653–665 doi:10.1017/S0007114521001318

Bacillus amyloliquefaciens ameliorates high-carbohydrate diet-induced metabolic phenotypes by restoration of intestinal acetate-producing bacteria in Nile Tilapia

Rong Xu[1], Miao Li[1], Tong Wang[1], Yi-Wei Zhao[1], Cheng-Jie Shan[1], Fang Qiao[1], Li-Qiao Chen[1], Wen-Bing Zhang[2], Zhen-Yu Du[1] and Mei-Ling Zhang[1]*

[1]*School of Life Sciences, East China Normal University, Shanghai 200241, People's Republic of China*
[2]*The Key Laboratory of Mariculture, Ministry of Education, The Key Laboratory of Aquaculture Nutrition and Feeds, Ministry of Agriculture, Ocean University of China, Qingdao 266003, People's Republic of China*

(Submitted 5 December 2020 – Final revision received 8 March 2021 – Accepted 12 April 2021 – First published online 16 April 2021)

Abstract

Poor utilisation efficiency of carbohydrate always leads to metabolic phenotypes in fish. The intestinal microbiota plays an important role in carbohydrate degradation. Whether the intestinal bacteria could alleviate high-carbohydrate diet (HCD)-induced metabolic phenotypes in fish remains unknown. Here, a strain affiliated to *Bacillus amyloliquefaciens* was isolated from the intestine of Nile tilapia. A basal diet (CON), HCD or HCD supplemented with *B. amy SS1* (HCB) was used to feed fish for 10 weeks. The beneficial effects of *B. amy SS1* on weight gain and protein accumulation were observed. Fasting glucose and lipid deposition were decreased in the HCB group compared with the HCD group. High-throughput sequencing showed that the abundance of acetate-producing bacteria was increased in the HCB group relative to the HCD group. Gas chromatographic analysis indicated that the concentration of intestinal acetate was increased dramatically in the HCB group compared with that in the HCD group. Glucagon-like peptide-1 was also increased in the intestine and serum of the HCB group. Thus, fish were fed with HCD, HCD supplemented with sodium acetate at 900 mg/kg (HLA), 1800 mg/kg (HMA) or 3600 mg/kg (HHA) diet for 8 weeks, and the HMA and HHA groups mirrored the effects of *B. amy SS1*. This study revealed that *B. amy SS1* could alleviate the metabolic phenotypes caused by HCD by enriching acetate-producing bacteria in fish intestines. Regulating the intestinal microbiota and their metabolites might represent a powerful strategy for fish nutrition modulation and health maintenance in future.

Key words: **Nile tilapia: High carbohydrate: Metabolic phenotypes: Intestinal microbiota regulation: SCFA**

With the increasing cost and limited supply of fishmeal in aquaculture, the utilisation of non-protein energy is becoming increasingly important[1]. Carbohydrates are one of the most abundant and cost-effective energy sources[2]. It is commonly accepted that appropriate levels of carbohydrates incorporated into fish diets will decrease the catabolism of protein and lipids to allow for protein-sparing effects[3]. However, teleost fish are generally considered to be glucose intolerant[4]. An excess proportion of carbohydrates in their diet causes metabolic disturbance, including decreased growth performance[5], persistent hyperglycaemia[6] and excess lipid deposition[7,8]. The glucose regulation mechanism in fish has been discussed in numerous studies; however, until now, most metabolic genes related to carbohydrate/glucose utilisation have been found to be conserved in vertebrates[9]. These studies suggested that in research on the carbohydrate metabolism characteristics in fish, we need to consider the function of the gut microbiota, which is closely related to host nutrition and metabolism and is referred as the 'second genome'[10].

The intestinal microbiota harbours multiple enzymes for the degradation and fermentation of dietary carbohydrates. Two *Bacteroides* strains, *Bacteroides intestinalis* and *Bacteroides ovatus*, are particularly enriched in genes encoding enzymes for the digestion of carbohydrates[11]. *Ruminococcus bromii* possesses a superior degradative ability with respect to resistant starch, and the released products from resistant starch can be utilised by other gut bacteria to produce SCFA, which have wide-ranging impacts on host physiology, including serving as an energy source for host cells or stimulating the production of gut hormones[12,13].

Abbreviations: GLP-1, glucagon-like peptide-1; HCB, high-carbohydrate diet supplemented with Bacillus amyloliquefaciens; HCD, high-carbohydrate diet; OTU, operational taxonomic unit; p38 MAPK, p38 mitogen-activated protein kinases; PI3K, phosphatidylinositol 3-kinase; p-mTOR, phosphorylated mechanistic target of rapamycin; qRT-PCR, quantitative real-time PCR.

* **Corresponding author:** Mei-Ling Zhang, email mlzhang@bio.ecnu.edu.cn

British Journal of Nutrition

A high-carbohydrate diet (HCD) altered the faecal microbiome by increasing the carbohydrate degradation members and SCFA excretion in humans[14]. However, a study in the grass carp (*Ctenopharyngodon idellus*) showed that SCFA level was lower in the hindgut when they were fed with a high-fibre/low-protein diet compared with those fed with a high-protein/low-fibre diet[15], indicating that the gut microbiota in the grass carp, which is a predominantly herbivorous fish, does not tend to ferment fibre to SCFA. These results suggested that the limited utilisation efficiency of carbohydrates by the intestinal microbiota might account for the glucose intolerance of fish.

The intestinal microbiota shows a great potential for maintaining glucose homoeostasis; however, the response to regulation by the intestinal microbiota in the context of glucose homoeostasis is strongly linked with the baseline microbiota composition. Research on humans with prediabetes showed that exercise-induced changes in the gut microbiota correlated with improved glucose metabolism and insulin sensitivity[16]. The microbiome of responders exhibited an enhanced capacity to produce SCFA and catabolise branched-chain amino acids, suggesting that the gut microbiota is a key determinant for the variability of glycaemic control[16]. A similar observation was made in a cohort of healthy individuals exposed to barley kernel-based bread, which suggested that humans harbouring a higher *Prevotella*:*Bacteroides* ratio exhibited improved glucose metabolism following 3-d consumption of barley kernel-based bread[17]. Fish harbour a *Proteobacteria*-dominated microbiota, which is different from the dominant microbiota in human or mice[18,19]. Whether regulation of the intestinal microbiota could increase the carbohydrate utilisation efficiency and alleviate the adverse effects caused by HCD in fish remains unknown.

Nile tilapia (*Oreochromis niloticus*) is an economically important fish species and is an ideal fish model for nutritional and metabolic studies because of its fast growth, high resistance to disease and available genomic information[20]. In the present study, we isolated a strain that could degrade starch *in vitro* from the intestine of Nile tilapia. 16S rRNA gene sequencing showed that the strain was affiliated to *Bacillus amyloliquefaciens* (designated as *B. amy SS1*). Three diet treatments, including control diet (CON), HCD and HCD supplemented with *B. amy SS1* (HCB), were used to feed Nile tilapia for 10 weeks. The host physiology and metabolic characteristics were identified in these three groups, and the possible mechanism by which *B. amy SS1* regulates carbohydrate utilisation was investigated.

Methods

Animal ethics

All experiments were conducted under the Guidance of the Care and Use of Laboratory Animals in China. This study was approved by the Committee on the Ethics of Animal Experiments of East China Normal University (F20190101).

Bacteria isolation

Healthy Nile tilapia were anaesthetised using MS-222. The fresh intestinal content was aseptically collected, then plated on a starch agar medium after gradient dilution and cultured at 28°C overnight. The colonies with a larger transparent zone after dropping with Lugol's iodine solution on the plates were picked and inoculated into the LB broth medium. The genomic DNA of the strain was extracted using a bacterial genome DNA extraction kit (Tiangen, DP302) according to the manufacturer's protocol. 16S rRNA was then amplified using primers 27F (5′-AGAGTTTGATCCTGGCTCAG-3′) and 1492R (5′-GGTTACCTTGTTACGACTT-3′). The PCR was performed using the following programme: 94°C for 5 min; 35 cycles at 94°C for 30 s, 55°C for 30 s and 72°C for 90 s; and 72°C for 10 min. The 16S rRNA gene was sequenced by Majorbio Bio-Pharm Technology Co. Ltd. 16S rRNA sequences were blast in GenBank (http://blast.ncbi.nlm.nih.gov/Blast.cgi). A phylogenetic tree was constructed using the neighbour-joining method in MEGA 7.0. The 16S rRNA gene sequence was submitted to GenBank (NCBI) with the accession number MT226660.

Detection of amylase activities

The amylase activity of the bacterium was detected as described previously[21]. In brief, a 1·0-ml LB broth culture, as a crude enzyme source, was reacted with 4·0 ml of substrate solution (1 % starch solution) at 45°C for 30 min. The enzyme reaction was interrupted by the addition of 1 ml 3,5-dinitrosalicylic acid reagent (Leagene, TC0030). The reaction solution was heated for 5 min in boiling water and then cooled in running tap water. The solution was constant volume to 10 ml, and then the OD540 was detected.

Preparation of high-carbohydrate diet supplemented with Bacillus amyloliquefaciens *diet*

B. amy SS1 was cultured in LB broth at 28°C at 220 rpm for 18 h. The cells were collected by centrifugation (12 000 ***g*** for 15 min) and resuspended in sterile water. The bacterial quantity was detected by serial dilution and counting on LB agar plates. B. *amy SS1* was mixed with the diet powder to make the pellets, and the final concentration of *B. amy SS1* was 10^7 CFU/g diet. The diet was made every 3 d and kept at 4°C.

Measurement of SCFA

SCFA concentrations were determined using GC. First, 200 µl bacteria solution was mixed with 0·1 ml of 50 % sulphuric acid and vortexed for 30 s. For intestinal SCFA measurement, 0·1 g of intestinal content was homogenised with 0·2 ml of water for 2 min. Then, 0·4 ml of pre-cooled ether was added to the mixture and vortexed for 30 s. The mixture was centrifuged at 12 000 ***g*** for 10 min at 4°C. The ether phase was detected in a GC under the following conditions: An initial column temperature of 100°C, held for 2 min, increased at a rate of 5°C/min to 180°C, and then held for 2 min; the flow rate was kept at 1 ml/min; the inlet temperature was set to 220°C and the sample amount was 1 µl with nitrogen as the carrier gas.

Animal experiments

Expt 1. Nile tilapia juveniles were obtained from Shanghai Ocean University (Shanghai, China). All fish were acclimated

Table 1 Formulations of the diets in Expt 1*

Ingredients	CON	HCD	HCB
Casein (g/kg)	320	320	320
Gelatin (g/kg)	80	80	80
Soyabean oil (g/kg)	70	70	70
Maize starch (g/kg)	300	450	450
Vitamin premix* (g/kg)	10	10	10
Mineral premix† (g/kg)	10	10	10
$Ca(H_2PO_4)_2$ (g/kg)	10	10	10
Carboxymethylcellulose (g/kg)	25	25	25
Cellulose (g/kg)	167·75	17·75	17·75
Choline chloride (g/kg)	5	5	5
Dimethyl-β-propiothetin (g/kg)	2	2	2
Butylated hydroxytoluene (g/kg)	0·25	0·25	0·25
B. amy SS1 (CFU/g)	0	0	10^7
Total quantity (g)	1000	1000	1000
Proximate composition (%)			
DM (%)	89·24	88·02	88·02
Protein (%)	35·89	35·09	35·09
Fat (%)	5·57	5·71	5·71

* Mixed vitamin (mg or IU/kg): 500 000 IU, vitamin A, 50 000 IU, vitamin D_3, 2500 mg vitamin E, 1000 mg vitamin K_3, 5000 mg vitamin B_1, 5000 mg vitamin B_2, 5000 mg vitamin B_6, 5000 mg vitamin B_{12}, 25 000 mg Inositol, 10 000 mg Pantothenic acid, 100 000 mg Cholin, 25 000 mg Niacin, 1000 mg folic acid, 250 mg biotin, 10 000 mg vitamin C.
† Mixed minerals (g/kg): 147.4 g $MgSO_4 \cdot 7H_2O$; 49.8 g NaCl; 10.9 g Fe (II) gluconate; 3.12 g $MnSO_4 \cdot H_2O$; $ZnSO_4 \cdot 7H_2O$; 0.62 g $CuSO_4 \cdot 5H_2O$; 0.16 g KI; 0.08 g $CoCl_2 \cdot 6H_2O$; 0.06 g NH_4 molybdate; 0.02 g $NaSeO_3$.

at 28 (SEM 1) °C and fed with a commercial diet (Tongwei, China) twice per day for 2 weeks. After acclimation, 225 uniformly sized fish (1·63 (SEM 0·05) g) were randomly distributed into three groups (three replicates for each group, twenty-five fish per replicate), including a control diet (CON), a HCD and a HCB. All fish were fed twice daily (08.30 and 20.30 hours) at a feeding rate of 4 % body weight. The formulation of the diets is listed in Table 1. The total weight of fish in each tank was recorded every 2 weeks.

Expt 2. Four treatments were set up in the second trial: HCD; HCD with a low dose of sodium acetate (900 mg/kg) (HLA); HCD with a medium dose of sodium acetate (1800 mg/kg) (HMA) and HCD with high dose of sodium acetate (3600 mg/kg) (HHA). Three replicates were set for each treatment, and each replicate contained twenty-five fish. The formulations of the diets are listed in online Supplementary Table S1.

Biochemical analysis

Glycogen, hexokinase, phosphofructokinase, pyruvate kinase, glycogen, TAG, NEFA, total cholesterol and LDL were detected using biochemical assay kits (Nanjing Jiancheng Bioengineering Institute) according to the manufacturer's instructions. Glucagon-like peptide-1 (GLP-1) was analysed by using an ELISA kit (Hengyuan Biotechnology).

Glucose tolerance test

The glucose tolerance test was performed after 24 h of fasting, followed by an intraperitoneal injection of D-glucose (500 mg/kg BW, 20 % in 0·85 % NaCl) (Sigma). The blood glucose levels at time 0, 0·5, 1·5 and 3 h after intraperitoneal injection were detected using an OneTouch glucometer (Bayer). The concentrations of fasting insulin in serum were analysed using an ELISA kit (Hengyuan Biotechnology).

Histological analysis

Liver and adipose tissues were fixed in 4 % paraformaldehyde, followed by gradient ethanol dehydration and xylene transparency procedure, then the tissues were embedded in paraffin and sliced into 5-μm sections for haematoxylin–eosin staining. For oil red O staining, liver tissue was embedded in optimum cutting temperature compound (Sakura) and immediately frozen at −80°C. Approximately 5–10 μm sections were gently flushed with 60 % isopropanol for a few seconds. Frozen liver sections were stained with oil red O and counterstained with haematoxylin to visualise the lipid droplets. The histological features were observed and captured under a light microscope (Nikon). Quantification and statistical analysis were conducted by using Image J.

16S rRNA amplicon sequencing

Genomic DNA extraction from intestinal contents was performed using an E.Z.N.A.® Soil DNA Kit (OMEGA) according to the manufacturer's instructions. DNA quantity and quality were measured using a NanoDrop 2000 Spectrophotometer (Thermo). The V3–V4 region of the bacteria 16S rRNA gene was amplified by PCR using primers 338F (5′-ACTCCTAC GGGAGGCAGCA-3′) and 806R (5′-GGACTACHVGGGTWT CTAAT-3′). Unique eight-base barcodes were added to each primer to distinguish the different PCR products. The PCR were performed in a 20 ml mixture containing 4 ml of 5 × Fast Pfu Buffer, 2 ml of 2·5 mM dNTP, 0·8 ml of each primer (5 mM), 0·4 ml of FastPfu Polymerase (TransGen) and 10 ng of template DNA. The PCR conditions were as follows: 95°C for 3 min; followed by 95°C for 30 s, 55°C for 30 s and 72°C for 45 s for 29 cycles; and extension at 72°C for 10 min. Purified PCR products were subjected to Illumina-based high-throughput sequencing (carried out by Majorbio Bio-Pharm Technology, Co. Ltd). The raw pair-end reads were subjected to quality-control procedures using Quantitative Insights Into Microbial Ecology (version 1.17). The qualified reads were clustered to generate operational taxonomic units (OTU) at the 97 % similarity level using UPARSE (version 7.1). Chimeric sequences were identified and removed using UCHIME (version 4.1). Taxonomic richness and diversity estimators were determined using the Mothur software. Principal coordinates analysis and heat-map analysis were performed in a MATLAB R2016a environment. Forty-six OTU were selected for heat-map analysis based on: (1) the abundances of these OTU were higher than 0·01% in each sample and (2) the abundance of these OTU was significantly different among groups as assessed using the one-way ANOVA with Tukey's adjustment analysis. The high-throughput sequencing data of intestinal microbiota are available in the NCBI short read archive (https://www.ncbi.nlm.nih. gov/sra) with the BioProject accession number PRJNA615286.

Quantitative real-time PCR analysis

The total RNA was isolated from tissues by using the TRIzol Reagent. The total RNA concentration was measured using a

NanoDrop 2000C spectrophotometer. RNA with an absorbance ratio OD 260/280 between 1·9 and 2·2 and an OD 260/230 >2·0 was used for subsequent analysis. As the template, 800 ng of total RNA was used to synthesise cDNA using a PrimeScript™ RT Reagent Kit (Takara) in a S1000TM Thermal Cycler (Bio-Rad). The primers for quantitative real-time PCR (qPCR) analysis were designed at NCBI, and the sequences are shown in online Supplementary Table S2. *β-actin* and *ef1α* were used as the reference genes. The qPCR volume was 25 μl containing 2·0 μl of cDNA template, 12·5 μl of 2 × SYBR qPCR Mixture (Aidlab), 2·0 μl of PCR primers (5 μM) and 6·5 μl of nuclease-free water and was performed in a CFX96 Connect Real-Time System (Bio-Rad). The qPCR conditions consisted of one cycle at 95°C for 30 s, followed by 40 cycles at 95°C for 5 s and an annealing step at 60°C for 20 s. Melting curves of the amplified products were generated to ensure the specificity of the assays at the end of each qPCR run. The relative gene expression values were calculated by using the $2^{-\Delta\Delta CT}$ method[22].

Western blot analysis

Radio immunoprecipitation assay (Beyotime Biotechnology) containing 1 mM PMSF (Beyotime Biotechnology) was used to extract proteins from liver tissues. Protein concentrations were measured using a BCA Protein Assay Kit (Beyotime Biotechnology). Forty micrograms of protein was subjected to SDS-PAGE, and the separated proteins were transferred to a nitrocellulose membrane. The membrane was blocked with 5 % BSA. Proteins on the membrane were reacted with the indicated antibodies in online Supplementary Table S3. Then, the membranes were further incubated with the anti-Rabbit IgG (Catalogue no. 926-32211; LI-COR Biosciences Corporate). GAPDH was used as a reference. The detection was achieved by using the Odyssey CLx Imager (Li-cor). The target proteins were quantified by using ImageJ software (National Institutes of Health).

Statistical analysis

Statistical analysis of all data was performed using SPSS software version 19 (IBM SPSS). The results are presented as mean values and standard errors of the mean. Data sets were assessed using one-way ANOVA with Tukey's adjustment. In the figures: $^{*}P < 0{\cdot}05$; $^{**}P < 0{\cdot}01$; $^{***}P < 0{\cdot}001$.

Results

A strain isolated from the intestine of Nile tilapia improved the growth performance of fish

16S rRNA gene sequencing showed that a strain with the ability to degrade starch was affiliated to *Bacillus amyloliquefaciens* ATCC 39320 (Fig. 1(a)). The selected strain was named *B. amy SS1* in the present study. *B. amy SS1* has a higher amylase activity *in vitro* (Fig. 1(b)) and could ferment maize starch to mainly produce acetate and butyrate (Fig. 1(c)).

To detect whether the addition of *B. amy SS1* could influence the growth performance of fish, three treatments, including CON, HCD and HCB, were used to feed fish for 10 weeks. The results showed that body weight was significantly higher in the HCD group than in the CON group; moreover, the average weight was further increased in the HCB group (Fig. 1(d)). Addition of *B. amy SS1* to the HCD resulted in the highest weight gain among the three groups (Fig. 1(e)), and the feed efficiency was higher in the HCB group compared with that in the HCD group (Fig. 1(f)).

The addition of Bacillus amyloliquefaciens to high-carbohydrate diet maintained the glucose homoeostasis

One of the metabolic phenotypes caused by HCD is the persistent hyperglycaemia in fish(6,23). To address whether the addition of *B. amy SS1* to HCD had a metabolic protective effect, the fasting glucose levels were detected. The results showed that the addition of *B. amy SS1* reduced the fasting glucose level caused by HCD (Fig. 2(a)). The glucose tolerance test showed that the addition of *B. amy SS1* markedly reduced the persistently higher blood glucose level caused by the HCD (Fig. 2(b) and (c)), that is, *B. amy SS1* improved glucose tolerance. Considering the important role of insulin in glucose homoeostasis, the fasting insulin level was detected; however, no significant difference was found among the groups (Fig. 2(d)), suggesting that the addition of *B. amy SS1* to the HCD might elevate insulin sensitivity rather than its amount. Glucose homoeostasis induced by *B. amy SS1* was further supported by significantly decreased liver glycogen levels (Fig. 2(e)). To investigate whether the insulin signalling pathway was activated by the addition of *B. amy SS1*, the expression levels of crucial proteins in the liver, including phosphatidylinositol 3-kinase (PI3K) and protein kinase B (AKT), were detected using Western blotting. The total levels of PI3K and AKT were similar among the groups; however, the levels of phosphorylated PI3K and AKT were significantly increased by *B. amy SS1* administration (Fig. 2(f) and (g)), suggesting that the addition of *B. amy SS1* to the HCD activated the PI3K/AKT insulin signalling pathway.

Enhanced glycolysis might improve glucose homoeostasis; therefore, three key enzymes of glycolysis, hexokinase, phosphofructokinase and pyruvate kinase, were analysed. The glycolytic enzyme activities in the liver were all increased in *B. amy SS1*-treated fish (Fig. 2(h)–(j)). The mRNA expression of glycolysis targeted genes, including *gck*, *pfk*, *pk* and *ir* in the liver, was down-regulated in the HCD group, but up-regulated by the addition of *B. amy SS1* (Fig. 2(k)). These data strongly suggested that the addition of *B. amy SS1* to the HCD enhanced glycolysis by activating the key enzymes related to glycolysis in the liver.

The addition of Bacillus amyloliquefaciens to high-carbohydrate diet reduced lipid deposition

HCD causes excess lipid accumulation in fish, which further aggravates the metabolic imbalance[24]. The HSI was mostly increased in the HCD group compared with that in the CON group, and the HCB group showed a decreased trend in HSI, although no significant difference was detected (Fig. 3(a)). The hepatic lipid content was significantly increased in the HCD group compared with that in the CON group, but it was decreased by the addition of *B. amy SS1* (Fig. 3(b)). The addition of *B. amy SS1* to the HCD also exhibited protective effects

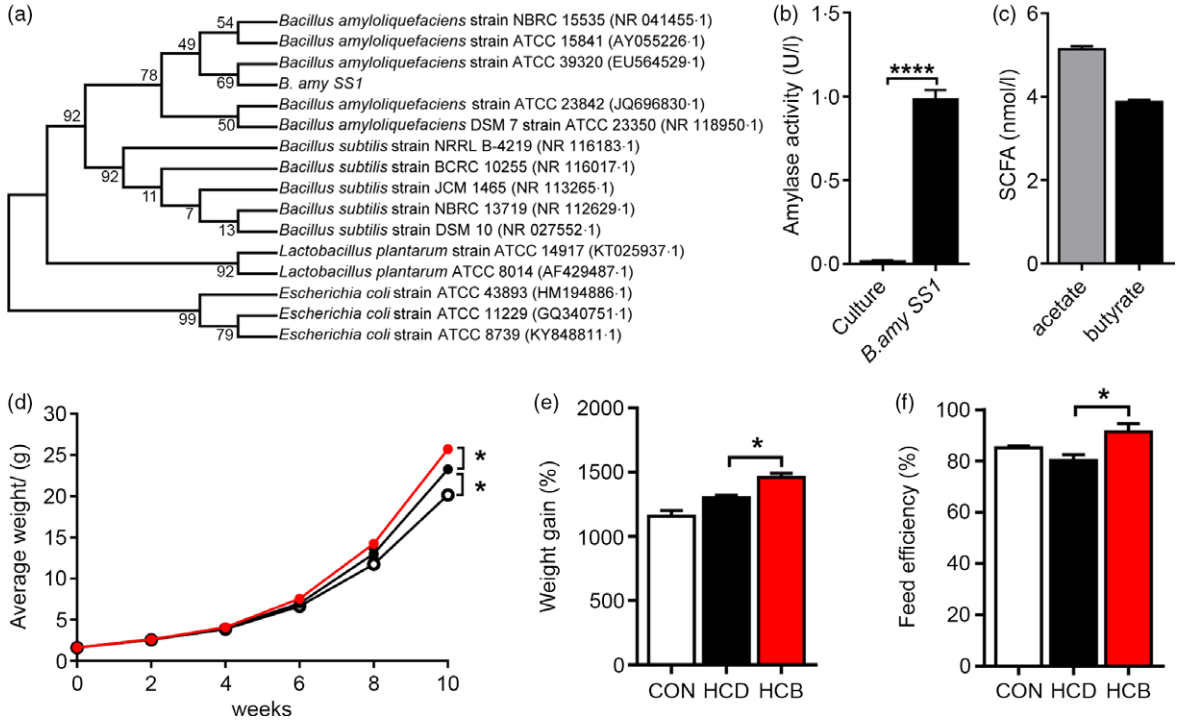

Fig. 1 Characteristics of *Bacillus amyloliquefaciens* isolated from intestine of Nile tilapia *in vitro* and *in vivo*. (a) Phylogenetic tree of *B. amy SS1*. (b) Amylase activity of *B. amy SS1 in vitro*. (c) SCFA production ability of *B. amy SS1 in vitro*. (d) Average weight, average weight (g) = total body weight/total tails. (e) Weight gain, weight gain (%) = 100 × (final fish weight – initial fish weight)/initial fish weight. (f) Feed efficiency, feed efficiency (%) = 100 × (final fish weight – initial fish weight)/feed intake. Data are expressed as mean values with their standard errors (*n* 3 groups). One-way ANOVA with Tukey's adjustment was used for data analysis. ⊖ CON; ⊖ high-carbohydrate diet (HCD); ⊖ high-carbohydrate diet supplemented with *Bacillus amyloliquefaciens* (HCB).

against HCD-induced liver damage, including lower content of TAG, NEFA and total cholesterol in the liver (Fig. 3(c)–(e)). Furthermore, haematoxylin–eosin and oil red O staining also indicated that the addition of *B. amy SS1* to the HCD markedly reduced lipid accumulation (Fig. 3(f)–(i)). The mRNA levels of genes related to lipid synthesis, including *fas*, *acc*α, *dgat2* and *ppar*γ, showed no significant difference in the liver among the groups (Fig. 3(j)). However, compared with that in the HCD group, the HCB group showed substantial up-regulation of genes targeted to lipolysis, including *atgl*, *cpt1*, *hsl* and *ppar*α in the liver (Fig. 3(k)).

To address whether activated lipolysis was associated with energy homoeostasis, the levels of key proteins involved in this process were detected using Western blotting. The phosphorylation of acetyl CoA carboxylase, a rate-limiting enzyme of fatty acid synthesis, showed no significant difference among groups in the liver (Fig. 3(l) and (m)). However, the level of phosphorylated adenosine 5'-monophosphate activated protein kinase α, a key molecule in the regulation of biological energy metabolism, was markedly increased in *B. amy SS1*-treated fish (Fig. 3(l) and (m)). Taken together, these results demonstrated that HCD supplemented with *B. amy SS1* reduced lipid deposition via AMPK/ACC signalling pathway, which was likely to increase energy expenditure.

Besides lipid accumulation in the liver, we also detected the content of total lipid in the body. Notably, a decrease in the total lipid content was observed in the *B. amy SS1*-treated fish (Fig. 3(n)). Moreover, MFI was lower in HCB group compared with that in the HCD group (Fig. 3(o)). *B. amy SS1* administration also reduced the cell size of adipocytes (Fig. 3(p) and (q)). Meanwhile, the serum TAG, NEFA, total cholesterol and LDL levels were reduced by the addition of *B. amy SS1* to the HCD, whereas HDL levels increased markedly in the *B. amy SS1*-treated fish (Fig. 3(r)–(v)). Taken together, these results further demonstrated that the addition of *B. amy SS1* to the HCD reduced lipid deposition in the fish.

The addition of Bacillus amyloliquefaciens *to the high-carbohydrate diet activated the mechanistic target of rapamycin/S6 signalling pathway and increased the protein accumulation*

We further assessed the impact of *B. amy SS1* on body protein accumulation. The results showed that the addition of *B. amy SS1* to the HCD increased the carcass index and carcass protein content significantly (Fig. 4(a) and (b)). The mRNA expression of *mtor* and *s6*, which are related to protein synthesis, was detected. The results indicated that *mtor* was significantly up-regulated by *B. amy SS1* administration, but no significant difference was observed for *s6* among the groups (Fig. 4(c)). Western blotting analysis demonstrated that the levels of phosphorylated mechanistic target of rapamycin (p-mTOR) and S6 ribosomal protein increased significantly after the addition of *B. amy SS1* to the HCD; however, no significant difference was found in the total levels of these proteins (Fig. 4(d) and (e)). Overall, these data implied that the HCD supplemented with *B. amy*

British Journal of Nutrition

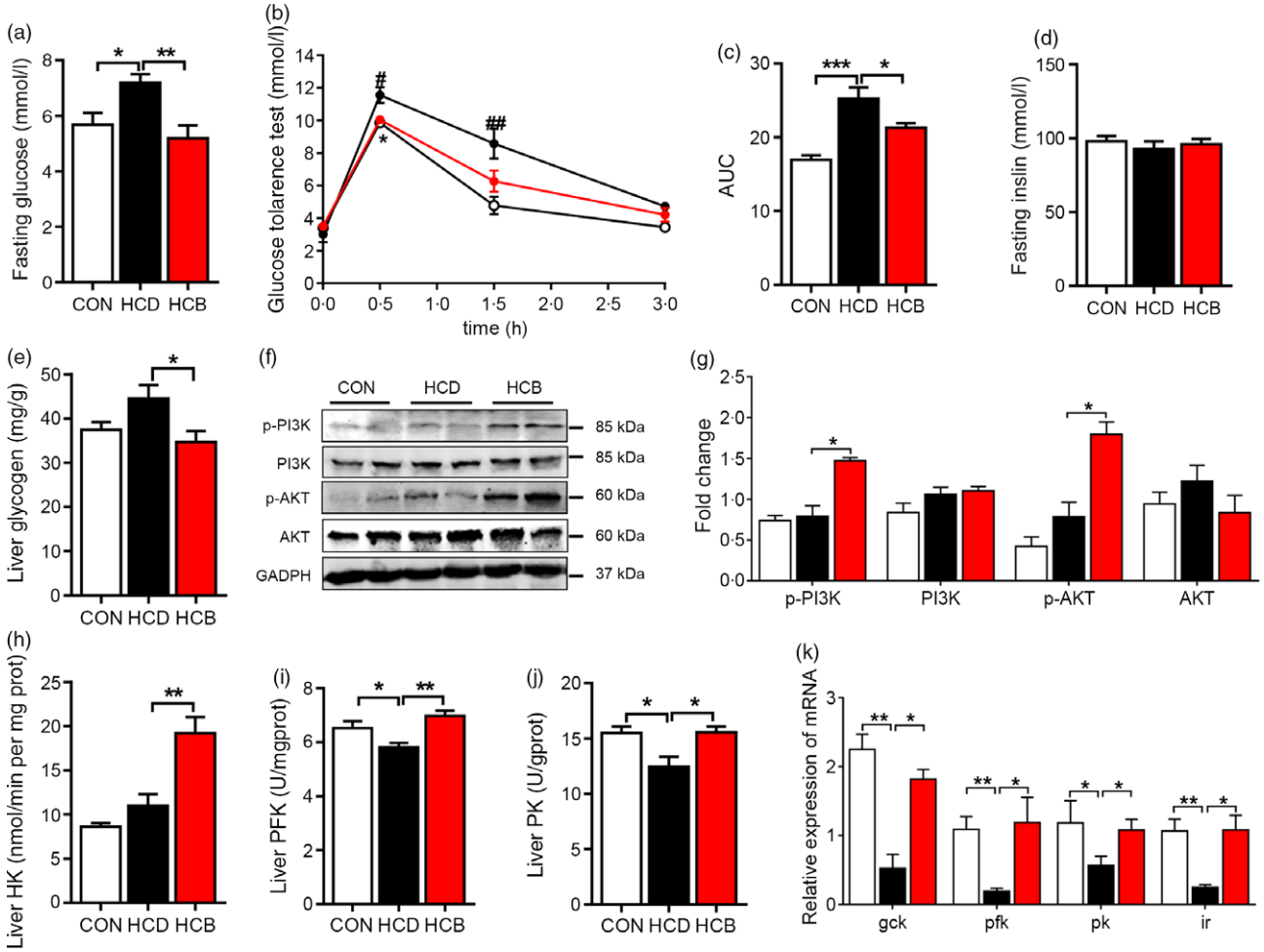

Fig. 2 *Bacillus amyloliquefaciens* improved glucose tolerance of Nile tilapia. (a) Fasting blood glucose concentration. (b) glucose tolerance test (GTT), glucose levels at 0 h, 0·5 h, 1·5 h and 3 h. (c) AUC of GTT, #: CON *v.* high-carbohydrate diet (HCD), #$P < 0·05$, ##$P < 0·01$; *HCD *v.* high-carbohydrate diet supplemented with *Bacillus amyloliquefaciens* (HCB): *$P < 0·05$. (d) Fasting insulin concentration. (e) Glycogen content in the liver. (f) Western blotting analysis of the levels of phosphorylated phosphatidylinositol 3-kinase (p-PI3K) and phosphorylated AKT (p-AKT) in the liver. (g) Quantitation of the levels of p-PI3K and p-AKT normalised to that of GAPDH. Glycolytic enzyme activities of hexokinase (HK) (h), phosphofructokinase (PFK) (i) and pyruvate kinase (PK) (j) in the liver. (k) Relative mRNA expression levels of *gck*, *pk*, *pfk*, and *ir* in the liver. Data are expressed as mean with their standard errors (*n* 6 fish). One-way ANOVA with Tukey's adjustment was used for data analysis. CON; HCD; HCB.

SS1 activated the mTOR/S6 signalling pathway and induced protein accumulation.

The addition of Bacillus amyloliquefaciens *to the high-carbohydrate diet altered the intestinal microbial community composition of Nile tilapia*

The gut microbiota has critical roles in host nutrition and metabolic processes. High-throughput sequencing was used to investigate the effects of *B. amy SS1* on the intestinal microbiota composition. Decreased Chao1, Ace, Sobs and Shannon-indexes in the HCD group were notably increased by *B. amy SS1* treatment (Table 2), suggesting that supplementation with *B. amy SS1* in the HCD restored the richness and diversity of the intestinal microbial community. To assess the overall composition of the bacterial community in the different groups, we analysed the microbiota composition at the phylum level. The intestinal microbiota was dominated by *Firmicutes*, *Proteobacteria*, *Bacteroidetes*, *Actinobacteria* and *Fusobacteria* in Nile tilapia (Fig. 5(a)). Compared with that in the CON group, the HCD group displayed a significant increase in the abundance of *Firmicutes*, while the addition of *B. amy SS1* to the HCD decreased the proportion of *Firmicutes* (Fig. 5(b)).

OTU-based principal coordinates analysis revealed that the HCD changed the intestinal microbiota compared with that of the CON group, while the addition of *B. amy SS1* modulated the microbiota composition, resulting in a composition similar to that of the CON group (Fig. 5(c)). The abundances of forty-six OTU in the HCD group showed significant differences among groups (Fig. 5(d)). Among these OTU, twelve were increased and thirty-four were decreased in the HCD group, while these OTU showed the opposite trend in the HCB group. OTU4496, OTU782 (*Streptococcus*), and OTU4496 (*Lactococcus*) were induced by the HCD, but were markedly reduced by the addition

British Journal of Nutrition

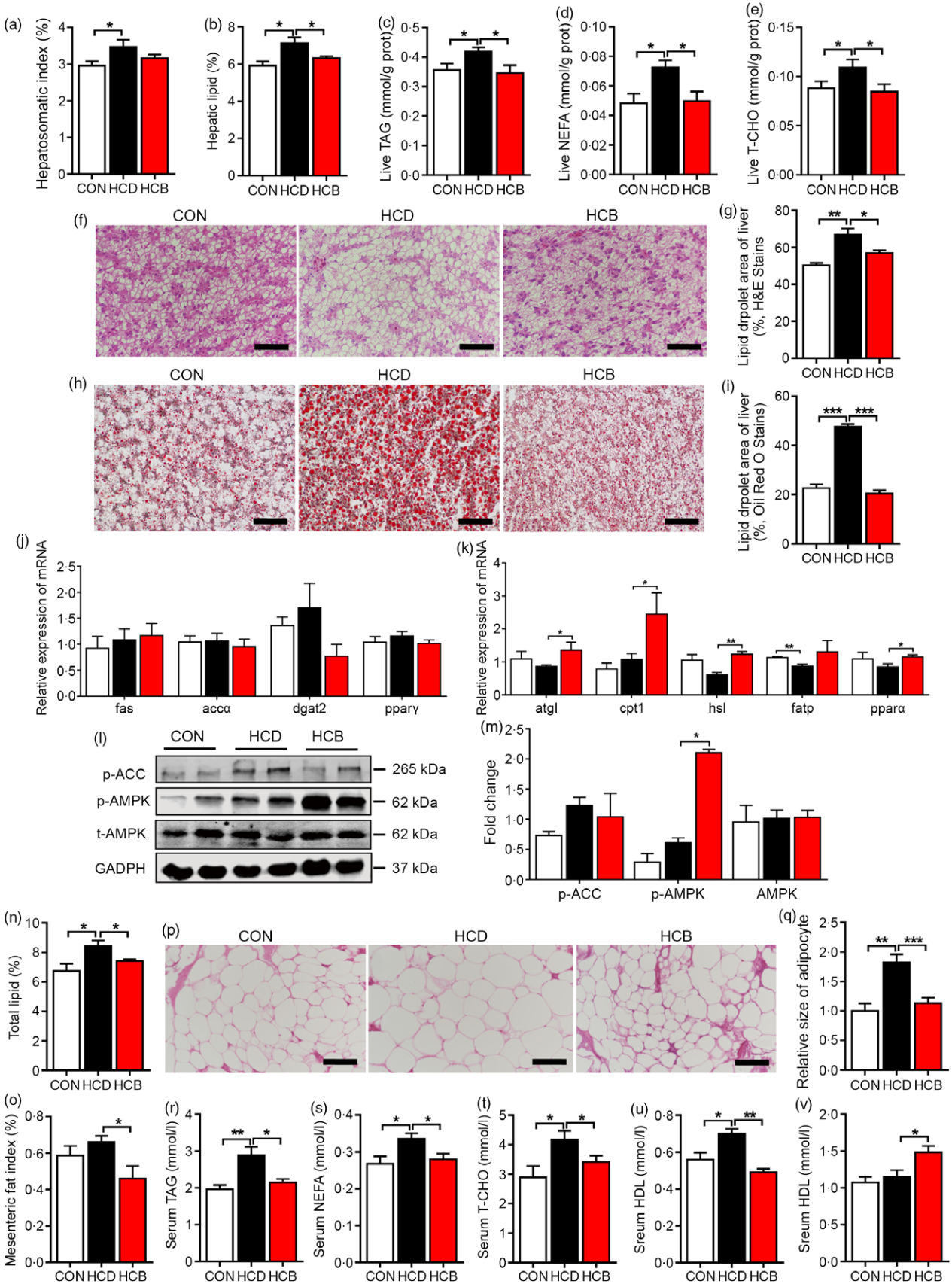

Fig. 3 *Bacillus amyloliquefaciens SS1* reduced lipid deposition of Nile tilapia. (a) HSI, HSI (%) = 100 × (Liver weight/body weight). (b) Hepatic lipid content. Content of TAG (c), NEFA (d) and total cholesterol (T-CHO) (e) in the liver. Histological analysis of liver (*n* 3 slides), liver tissue stained with haematoxylin–eosin (H&E) (f) and statistical analysis of lipid area percentage (g), liver tissue stained with oil red O (h) and statistical analysis of lipid area percentage (i), scale bar = 100 μm. Relative mRNA expression of genes related to lipid synthesis*: fas*, *accα*, *dgat2* and *pparγ* in the liver (j) and lipolysis: *atgl*, *cpt1*, *hsl*, *fatp* and *pparα* in the liver (k). (l) Western blotting analysis of the levels of phosphorylation of acetyl CoA carboxylase (p-ACC) and phosphorylated adenosine 5'-monophosphate activated protein kinase α (p-AMPK) in the liver. (m) Quantitation of the levels of p-ACC and p-AMPK normalised to that of GAPDH. (n) Total lipid content in the whole body of Nile tilapia at the end of the feeding trial. (o) MFI, MFI (%) = 100 × (Mesenteric fat weight/body weight). Histological analysis of fat tissue (*n* 3 slides), fat tissue stained with H&E (p) and relative size of adipocyte (q), scale bar = 100 μm. r-v Content of TAG (r), NEFA (s), T-CHO (t), LDL (u), and HDL (v) in serum. Data are expressed as mean with their standard errors (*n* 6 fish). One-way ANOVA with Tukey's adjustment was used for data analysis. □CON; ■high-carbohydrate diet (HCD); ■high-carbohydrate diet supplemented with *Bacillus amyloliquefaciens* (HCB).

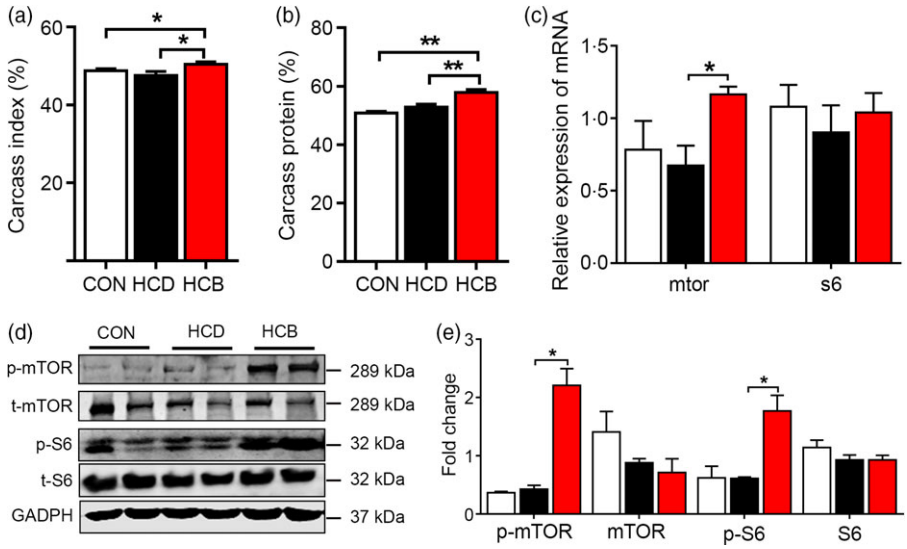

Fig. 4 *Bacillus amyloliquefaciens* increased protein accumulation of Nile tilapia. (a) Carcass index, Carcass index (%) = 100 × (Carcass weight/body weight). (b) Carcass protein content. (c) Relative mRNA expression of *mtor* and *s6* in the liver. (d) Western blotting analysis of the levels of phosphorylated mechanistic target of rapamycin (p-mTOR) and S6 ribosomal protein (p-S6) in the liver. (e) Quantitation of the levels of p-mTOR and p-S6 were normalised to that of GAPDH. Data are expressed as mean with their standard errors (*n* 6 fish). One-way ANOVA with Tukey's adjustment was used for data analysis. □ CON; high-carbohydrate diet ■ (HCD); ■ high-carbohydrate diet supplemented with *Bacillus amyloliquefaciens* (HCB).

Table 2 *Bacillus amyloliquefaciens* changed the intestinal microbial community abundance and diversity of Nile tilapia. Richness and diversity of the intestinal microbiota in three groups
(Mean values with their standard errors)*

	Sampling depth		Richness estimators						Diversity estimators			
	Mean sequence (bp)		Chao1		Ace		Sobs		Shannon		Simpson	
Groups	Mean	SEM	Mean	SEM	Mean	SEM	Mean	SEM	Mean	SEM	Mean	SEM
CON	36 712·67	997·39	2349·08	196·17	2400·35	206·14	2049·50	125·96	4·70	0·21	0·12	0·03
HCD	40 175·33	5277·25	1294·46†	864·86	1314·99†	881·63	1136·33†	742·07	3·80†	0·70	0·11	0·03
HCB	36 989·83	3169·76	2173·07‡	70·14	2187·67‡	68·70	1916·00‡	27·75	4·53‡	0·11	0·15	0·03

CON, control diet; HCD, high-carbohydrate diet; HCB, high-carbohydrate diet supplemented with *Bacillus amyloliquefaciens*.
* One-way ANOVA with Tukey's adjustment was used to detect the significant differences between groups. Different letters represent significant difference at $P < 0·05$.
† Represents the significant difference between CON and HCD.
‡ Represents the significant difference between HCD and HCB.

of *B. amy SS1*. Moreover, the HCD decreased the abundances of OTU209 (*Weisselia*); OTU6174 (*Romboutsia*); OTU938 (*Faecalibacterium*); OTU6929 and OTU2196 (*Ruminococcus*); OTU3573 (*Blautia*); OTU4850 and OTU4857 (*Prevotellaceae*); OTU5921, OTU4958 and OTU3077 (*Bacteroides*); and OTU6083 (*Bifidobacterium*), while the addition of *B. amy SS1* increased the abundances of these OTU. We noticed that these bacteria were commonly associated with SCFA production(25,26). Collectively, these results indicated that compared with that in the HCD group, the addition of *B. amy SS1* to the HCD restored the abundance of SCFA production bacteria in Nile tilapia.

The addition of Bacillus amyloliquefaciens *to the high-carbohydrate diet promoted the secretion of glucagon-like peptide-1*

The results of the previous section showed that the abundance of SCFA-producing bacteria was restored by *B. amy SS1* treatment; therefore, the concentration of SCFA in the intestines was determined. The result suggested that the reduced concentration of acetate in the HCD group was dramatically elevated by the addition of *B. amy SS1* (Fig. 5(e)). The propionate content was below the detection limit, and the content of butyrate showed marked intra-group difference (data not shown). The mRNA expression of *ffar2*, which encodes free fatty acid receptor 2 (the receptor of SCFA in fish), was notably up-regulated in the liver after the addition of *B. amy SS1* to the HCD (Fig. 5(f)).

Considering GLP-1 is the main target of FFAR2, the amounts of GLP-1 in the intestine and serum were detected. The results suggested that intestinal and serum GLP-1 levels increased significantly after the addition of *B. amy SS1* to the HCD (Fig. 5(g) and (h)). To determine how the signal is transduced, p38 mitogen-activated protein kinases (p38 MAPK), which regulates the production of GLP-1[27], was detected. The results showed that the level of phosphorylated p38 MAPK was evidently increased by *B. amy SS1* administration, although no significant difference of total p38 MAPK was observed among groups

British Journal of Nutrition

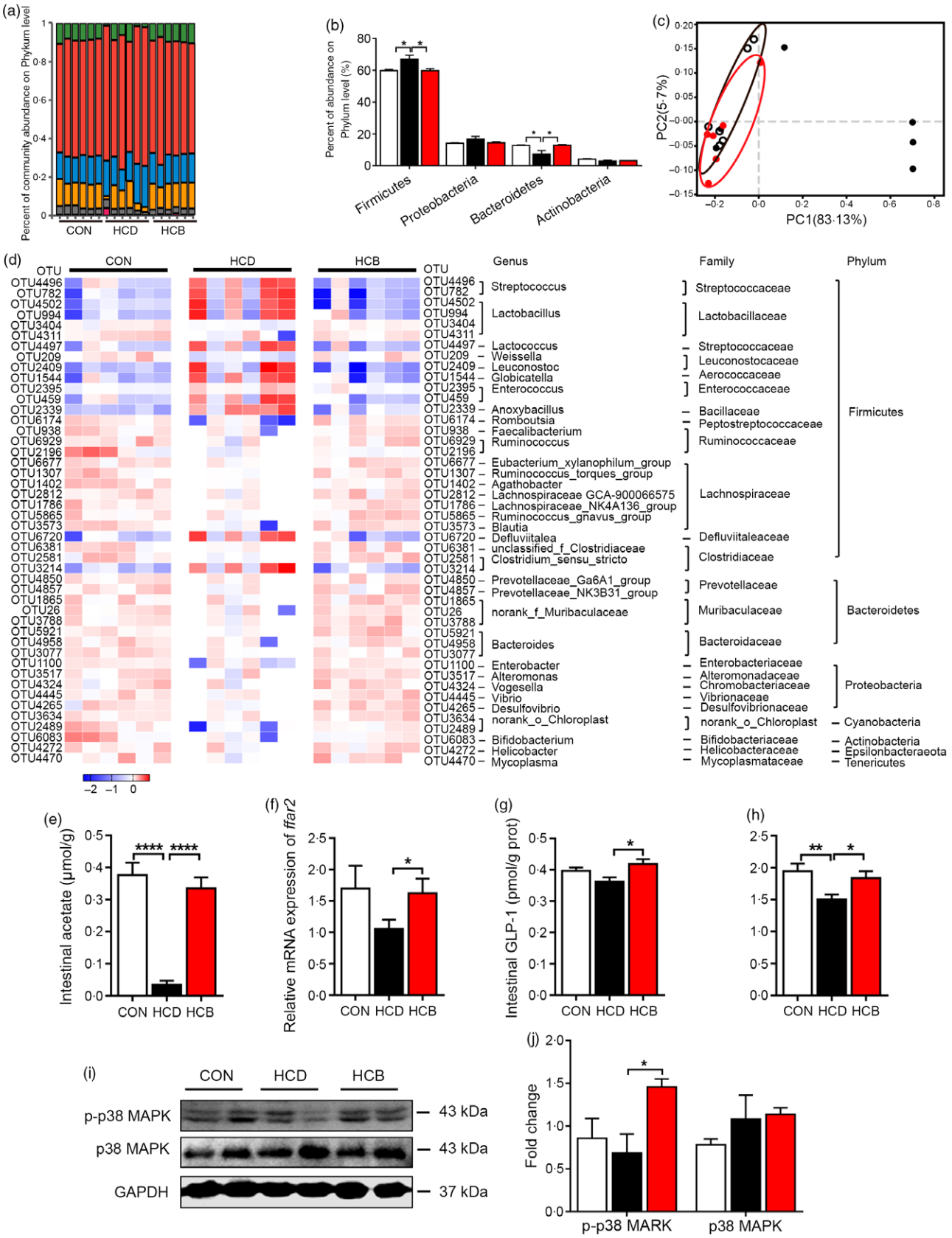

Fig. 5 *Bacillus amyloliquefaciens* altered the intestinal microbial community composition and microbial metabolites of Nile tilapia. (a) Percentage of community abundance at the phylum level. (b) Histogram of community abundance at the phylum level. (c) Principal coordinates analysis (PCoA) of the intestinal bacterial community. (d) Heat-map of the bacterial abundance in the intestine. (e) Acetate content in the intestine. (f) Relative mRNA expression of *ffar2* in the liver. Content of glucagon-like peptide-1 (GLP-1) in intestine (g) and serum (h). (i) Western blotting analysis of the levels of phosphorylated p38 mitogen-activated protein kinases (p-p38 MAPK) in the liver. (j) Quantitation of the levels of p-p38 MAPK normalised to that of GAPDH. Data are expressed as mean with their standard errors (*n* 6 fish). One-way ANOVA with Tukey's adjustment was used for data analysis. Firmicutes' Proteobacteria; Bacteroidetes; Actinobacteria; Fusobacteria; Others; ☐ CON; ■ high-carbohydrate diet (HCD); ■ high-carbohydrate diet supplemented with *Bacillus amyloliquefaciens* (HCB); –2; –1; 0.

(Fig. 5(i) and (j)). These data demonstrated that the increased production of acetate induced by the addition of *B. amy SS1* to the HCD might account for the increased secretion of GLP-1.

Addition of sodium acetate mimicked the effects of Bacillus amyloliquefaciens *supplementation of the high-carbohydrate diet*

To further verify the function of microbial metabolites, different concentrations of sodium acetate (HLA, 900 mg/kg; HMA, 1800 mg/kg and HHA, 3600 mg/kg) were added to the HCD to feed Nile tilapia for 8 weeks. The fasting glucose test and glucose tolerance test showed that blood glucose levels were obviously reduced in the HMA and HHA groups compared with those in the HCD group (Fig. 6(a)–(c)), suggesting that the addition of certain concentrations of sodium acetate to the HCD could improve glucose homoeostasis of fish. Additionally, the HSI was noticeably decreased in the HMA and HHA groups (Fig. 6(d)). In parallel, liver TAG levels were reduced in the HMA and HHA groups (Fig. 6(e) and (f)). Accordingly, liver histology via haematoxylin–eosin staining showed that the percentage of the lipid area exhibited was reduced substantially in the HMA and HHA groups compared with that in the HCD group (Fig. 6(g) and (h)). Importantly, we also found that GLP-1 levels were elevated in the serum from the HMA and HHA groups (Fig. 6(i)). Western blotting analysis revealed that levels of phosphorylated AKT and phosphorylated adenosine 5'-monophosphate activated protein kinase α increased significantly in the three sodium acetate supplementation groups, while the level of p-mTOR was only increased in the HMA and HHA groups (Fig. 6(j) and (k)), and these effects are dose-dependent. In brief, the addition of acetate could mimic the metabolic effects caused by addition of *B. amy SS1* to the HCD.

Discussion

Increasing research in humans and other vertebrates has shown that the intestinal microbiota plays an important role in carbohydrate degradation and fermentation[28,29]. In aquaculture, how to increase the carbohydrate utilisation efficiency and alleviate the metabolic phenotypes caused by HCD is vitally important. In the past, administration of benfotiamine and bile acids showed the potential to increase the carbohydrate utilisation efficiency in fish[30,31]; however, the influence of the intestinal microbiota on host carbohydrate metabolism is unknown. In the present study, *B. amy SS1* isolated from the intestine of Nile tilapia showed an ability to alleviate metabolic phenotypes caused by HCD by restoration of acetate-producing bacteria in the intestines, suggesting that modulation of the intestinal microbiota has the great potential to regulate the host metabolism of fish.

The intestinal microbiota produces key enzymes for carbohydrate degradation and fermentation to produced SCFA, which are considered to be beneficial to the host[11,32]. Consistent with previous research[15], we also found that the abundance of bacterial members closely related to SCFA production was decreased under HCD, suggesting that the HCD diminished the numbers of functional bacteria, which might be related to the metabolic phenotypes caused by the HCD in fish. The addition of *B. amy SS1* to the HCD restored the bacteria that are believed to be involved in the degradation of carbohydrates or production of SCFA. OTU209 is affiliated to *Weisells*, which is commonly expanded in a carbohydrate-rich setting and has the ability to ferment polysaccharides to produce SCFA[26,33]. OTU938 is affiliated to *Faecalibacterium*, which is one of the dominant bacteria in the hindgut with higher levels of SCFA in *Hermosilla azurea*[34]. An expansion of *Faecalibacterium* and significantly greater SCFA concentrations were found in the colon of pigs fed with a high-resistant starch diet[35]. The abundance of OTU6929 and OTU2196, belonging to *Ruminococcus*, was increased by the addition of *B. amy SS1* to the HCD. It has been reported that *Ruminococcus* could ferment resistant starch into SCFA[12,36]. OTU4850 and OTU4857 are affiliated to *Prevotellaceae*, which were increased in both humans and rats fed with higher dietary starch and are related to the increased SCFA production[25]. We also found that abundance of OTU6083, belonging to *Bifidobacterium*, was lower in the HCD group but enriched in the HCB group. The abundance of *Bifidobacteria* was increased in the human gut by supplementing the diet with resistant starch from potatoes[12].

The metabolic syndrome induced by HCD is hyperglycaemia and hepatic steatosis in mammals[37]. To determine the mechanism by which *B. amy SS1* alleviated these metabolic phenotypes in fish, we detected the key signalling pathways related to glucose and lipid metabolism. We found that acetate production increased in the intestines of Nile tilapia in HCB group compared with HCD group. Increased levels of SCFA stimulate GLP-1 production via the p38 MAPK signalling pathway[27], and in line with the previous research, our results showed higher level of p38 MAPK and GLP-1 in the HCB group. The important roles of GLP-1 in glucose homoeostasis and lipid metabolism have been well documented[38,39]. In mammals, GLP-1 decreases glucose levels via stimulation of insulin release and inhibition of nutrient absorption in the gastrointestinal tract. Meanwhile, in rainbow trout, it was reported that GLP-1 increased glucose levels via activation of glycogenolysis and gluconeogenesis in the liver[40]. Our results showed that GLP-1 improved glucose homoeostasis, which is consistent with findings in mice[41]. Although there was no difference in the insulin content among groups, the PI3K/AKT insulin signalling pathway was activated in the HCB group, which may relate to the improved glucose tolerance. Besides glucose homoeostasis, GLP1 also regulates lipid metabolism. GLP-1 suppresses hepatic lipogenesis via activation of the AMPK pathway in chicken and rats[27,42]. However, to date, there has been no study on the regulation of lipid metabolism by GLP-1 in fish. The results of the present study showed that GLP1 modulated the reduction of lipid deposition, which may be due to the increased lipid catabolism. Furthermore, the AMPK/ACC signalling pathway was activated in the HCB group, which is related to the energy expenditure[43]. Taken together, our results demonstrated that the addition of *B. amy SS1* to the HCD stimulated the GLP-1 signalling pathway, which is responsible for the

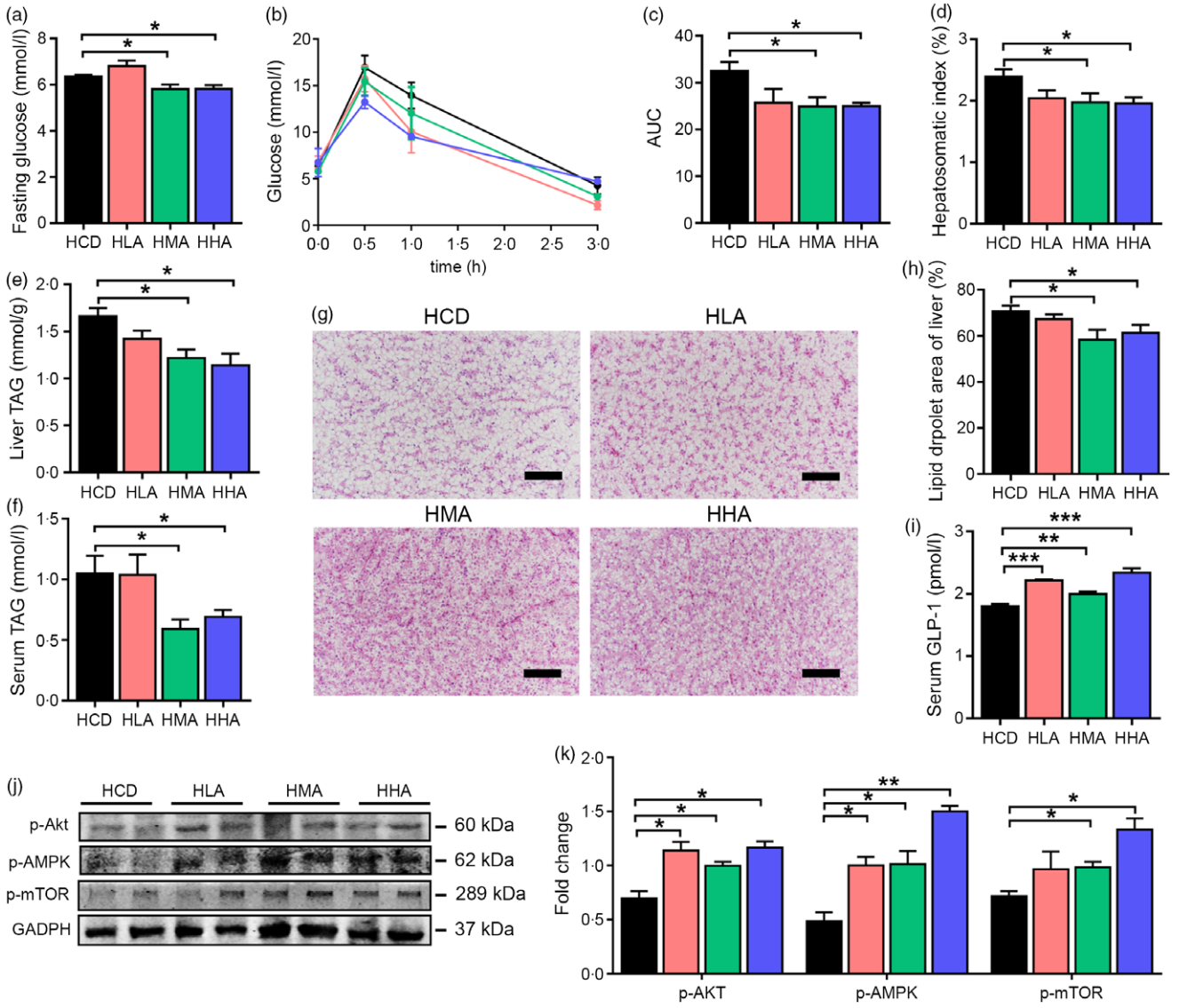

Fig. 6 Sodium acetate mirrored the metabolic benefits of *Bacillus amyloliquefaciens*. (a) Fasting blood glucose concentration. (b) glucose tolerance test (GTT), glucose levels at 0 h, 0·5 h, 1·5 h and 3 h. (c) AUC of GTT. (d) Serum glucagon-like peptide-1 (GLP-1). (e) HSI. Histological analysis of the livers (*n* 3 slides): liver tissues stained with H&E (f) and statistical analysis of lipid area percentage (g), scale bar = 100 μm. Content of TAG in the liver (h) and serum (i). (j) Western blotting analysis of the levels of phosphorylated p-AKT, p-AMPK and p-mTOR in the liver. (k) Quantitation of the levels of p-AKT, p-AMPK and p-mTOR was normalised to that of GAPDH. Data are expressed as mean with their standard errors (*n* 6 fish). One-way ANOVA with Tukey's adjustment was used for data analysis. high-carbohydrate diet —●— (HCD); —●— HLA; —●— HMA; —●— HHA.

alleviation of metabolic phenotypes in fish, suggesting a conserved function of GLP-1 in glucose homoeostasis and lipid metabolism between fish and other vertebrates.

It is important for fish to produce more body protein in aquaculture(44,45). Many attempts have been made to increase body protein levels in fish. It was reported that dietary methionine increased protein synthesis by improving amino acid metabolism in turbot (*Scophthalmus maximus L.*)[46]. In the same fish species, replacement of fishmeal by soyabean meal reduced protein synthesis via nutrient-sensing[47]. In the present study, our results showed that the addition of *B. amy SS1* to the HCD increased the carcass protein proportion in fish. Increased protein synthesis is commonly associated with activation of mTOR(48,49). Our results showed that the mTOR/S6 signalling pathway was activated in the HCB group. To our knowledge, this is the first study to show a relationship between the intestinal microbiota and protein accumulation in fish, suggesting that the intestinal microbiota might be a new target for protein synthesis in fish.

The benefits of sodium acetate have been reported extensively in animals, including improving growth performance, suppressing intestinal inflammation and maintaining energy homoeostasis(50,51). Previously, our laboratory found that the addition of sodium acetate could increase the acetate concentration in the intestine of Nile tilapia[51]. In the present study, the addition of sodium acetate to the HCD mirrored the beneficial metabolic effects of *B. amy SS1* supplementation. The addition of a certain concentration of sodium acetate to the HCD could

induce the production of GLP-1. It should be noted that phosphorylated mTOR levels were increased in the HMA and HHA groups, but no significant difference in the carcass protein content was found among treatments (data not shown). The possible reasons are that the increased protein accumulation might be induced by other microbial metabolites instead of acetate, or the feeding period should be prolonged.

Because juvenile tilapia was used in the present study, the potential effect of the growth stage on the intestinal microbiota and host metabolic characteristics has not been studied. In the present study, OTU6677 (*Eubacterium_xylanophilum_group*), OTU5865 (*Ruminococcus_gnavus_group*), OTU6381 (*Clostridiaceae_sensu_stricto*) and OTU1100 (*Enterobacter*) were decreased in HCD group compared with CON group, which may be related to the decreased content of cellulose in HCD. However, addition of *B. amy SS1* increased their abundance and alleviated the metabolic phenotypes caused by HCD, suggesting the important role of *B. amy SS1* in altering gut microbiota and regulating fish metabolism. It should be noted that the differences in diet components between CON and HCD included the increased maize starch and the decreased cellulose, and the potential influence of cellulose on intestinal microbiota and host metabolism still needed further investigation.

In summary, our study demonstrated that the addition of *B. amy SS1*, a bacterium affiliated to *Bacillus amyloliquefaciens*, in HCD could promote growth performance, improve glucose tolerance, reduce lipid deposition and increase protein accumulation in Nile tilapia. The addition of *B. amy SS1* to HCD rebuilt the microbiota composition, and especially, increased the abundance of acetate-producing bacteria in the intestines of fish. The addition of sodium acetate to the HCD mirrored the beneficial effects of *B. amy SS1* supplementation in ameliorating metabolic phenotypes. Collectively, this study enhanced our understanding of methods to alleviate metabolic phenotypes caused by HCD in fish by adding functional bacteria, which might represent a novel strategy to regulate fish metabolism.

Acknowledgements

This work was supported by the National Key R&D programme (grant number 2019YFD0900200 & 2018YFD0900400) and the National Natural Science Foundation of China (grant number 31972798).

All authors contributed experimental assistance and intellectual input to this study. M.-L. Z. and Z.-Y. D. conceived the original concept. M.-L. Z., Z.-Y. D. and L.-Q. C. designed the experimental strategies and sampling plans. R. X. and M. L. performed the feeding experiments. R. X., T. W. and C.-J. S. contributed to the collection of samples. R. X. and Y.-W. Z. performed the molecular and biochemistry detections. R. X. performed the bioinformatic analysis of the intestinal samples for microbial composition and the statistical analyses. M.-L. Z., Z.-Y. D., F. Q. and L.-Q. C. provided essential materials and technical supports. M.-L. Z., R. X. and W.-B. Z. drafted and revised the manuscript. All authors read and approved the final manuscript.

The authors declare that there are no conflicts of interest.

Supplementary material

For supplementary material referred to in this article, please visit https://doi.org/10.1017/S0007114521001318

References

1. Hardy RW (2010) Utilization of plant proteins in fish diets: effects of global demand and supplies of fishmeal. *Aquacult Res* **41**, 770–776.
2. Maas RM, Verdegem MCJ, Wiegertjes GF, *et al.* (2020) Carbohydrate utilisation by tilapia: a meta-analytical approach. *Rev Aquacult* **12**, 1851–1866.
3. Krogdahl Å, Hemre GI & Mommsen TP (2005) Carbohydrates in fish nutrition: digestion and absorption in postlarval stages. *Aquacult Nutr* **11**, 103–122.
4. Kamalam BS, Medale F & Panserat S (2017) Utilisation of dietary carbohydrates in farmed fishes: new insights on influencing factors, biological limitations and future strategies. *Aquaculture* **467**, 3–27.
5. Li JN, Xu QY, Wang CA, *et al.* (2016) Effects of dietary glucose and starch levels on the growth, haematological indices and hepatic hexokinase and glucokinase mRNA expression of juvenile mirror carp (*Cyprinus carpio*). *Aquacult Nutr* **22**, 550–558.
6. Kostyniuk DJ, Marandel L, Jubouri M, *et al.* (2019) Profiling the rainbow trout hepatic miRNAome under diet-induced hyperglycemia. *Physiol Genomics* **51**, 411–431.
7. Prisingkorn W, Prathomya P, Jakovlić I, *et al.* (2017) Transcriptomics, metabolomics and histology indicate that high-carbohydrate diet negatively affects the liver health of blunt snout bream (*Megalobrama amblycephala*). *BMC Genomics* **18**, 1–15.
8. Viegas I, Jarak I, Rito J, *et al.* (2016) Effects of dietary carbohydrate on hepatic de novo lipogenesis in European seabass (*Dicentrarchus labrax* L.). *J Lipid Res* **57**, 1264–1272.
9. Zhang Y, Qin C, Yang L, *et al.* (2018) A comparative genomics study of carbohydrate/glucose metabolic genes: from fish to mammals. *BMC Genomics* **19**, 246–246.
10. Jia W, Li H, Zhao L, *et al.* (2008) Gut microbiota: a potential new territory for drug targeting. *Nat Rev Drug Discovery* **7**, 123–129.
11. Zhang M, Chekan JR, Dodd D *et al.* (2014) Xylan utilization in human gut commensal bacteria is orchestrated by unique modular organization of polysaccharide-degrading enzymes. *Proc Natl Acad Sci USA* **111**, E3708–E3717.
12. Baxter NT, Schmidt AW, Venkataraman A, *et al.* (2019) Dynamics of human gut microbiota and short-chain fatty acids in response to dietary interventions with three fermentable fibers. *mBio* **10**, e02566.
13. Ze X, Duncan SH, Louis P, *et al.* (2012) *Ruminococcus bromii* is a keystone species for the degradation of resistant starch in the human colon. *ISME J* **6**, 1535–1543.
14. Fava F, Gitau R, Griffin BA, *et al.* (2013) The type and quantity of dietary fat and carbohydrate alter faecal microbiome and short-chain fatty acid excretion in a metabolic syndrome 'at-risk' population. *Int J Obes* **37**, 216–223.
15. Hao YT, Wu SG, Jakovlić I, *et al.* (2017) Impacts of diet on hindgut microbiota and short-chain fatty acids in grass carp (*Ctenopharyngodon idellus*). *Aquacult Res* **48**, 5595–5605.
16. Liu Y, Wang Y, Ni Y, *et al.* (2020) Gut microbiome fermentation determines the efficacy of exercise for diabetes prevention. *Cell Metab* **31**, 77–91.e75.
17. Kovatcheva-Datchary P, Nilsson A, Akrami R, *et al.* (2015) Dietary fiber-induced improvement in glucose metabolism is associated with increased abundance of prevotella. *Cell Metab* **22**, 971–982.

British Journal of Nutrition

18. Wang AR, Ran C, Ringø E, *et al.* (2018) Progress in fish gastrointestinal microbiota research. *Rev Aquacult* **10**, 626–640.
19. Bäckhed F, Ley RE, Sonnenburg JL, *et al.* (2005) Host-bacterial mutualism in the human intestine. *Science* **307**, 1915.
20. de Verdal H, Vandeputte M, Mekkawy W, *et al.* (2018) Quantifying the genetic parameters of feed efficiency in juvenile Nile tilapia *Oreochromis niloticus*. *BMC Genet* **19**, 105–105.
21. Bernfeld P (1955) Amylases, α and β. *Meth Enzymol* **1**, 149–158.
22. Livak KJ & Schmittgen TD (2001) Analysis of relative gene expression data using real-time quantitative PCR and the 2 −ΔΔCT method. *Methods* **25**, 402–408.
23. Conde-Sieira M, Salas-Leiton E, Duarte MM, *et al.* (2016) Short- and long-term metabolic responses to diets with different protein:carbohydrate ratios in Senegalese sole (*Solea senegalensis*, Kaup 1858). *Br J Nutr* **115**, 1896–1910.
24. Xie D, Yang L, Yu R, *et al.* (2017) Effects of dietary carbohydrate and lipid levels on growth and hepatic lipid deposition of juvenile tilapia, *Oreochromis niloticus*. *Aquaculture* **479**, 696–703.
25. Cherbuy C, Bellet D, Robert V, *et al.* (2019) Modulation of the caecal gut microbiota of mice by dietary supplement containing resistant starch: impact is donor-dependent. *Front Microbiol* **10**, 1234.
26. Sturino JM (2018) Literature-based safety assessment of an agriculture- and animal-associated microorganism: *Weissella confusa*. *Regul Toxicol Pharmacol* **95**, 142–152.
27. Zhang J-M, Sun Y-S, Zhao L-Q, *et al.* (2019) SCFAs-induced GLP-1 secretion links the regulation of gut microbiome on hepatic lipogenesis in chickens. *Front Microbiol* **10**, 2176.
28. He C, Wu Q, Hayashi N *et al.* (2020) Carbohydrate-restricted diet alters the gut microbiota, promotes senescence, shortens the life span in senescence-accelerated prone mice. *J Nutr Biochemistr* **78**, 108326.
29. Spring S, Premathilake H, DeSilva U, *et al.* (2020) Low protein-high carbohydrate diets alter energy balance, gut microbiota composition and blood metabolomics profile in young pigs. *Sci Rep* **10**, 1–15.
30. Xu C, Liu WB, Dai YJ, *et al.* (2017) Long-term administration of benfotiamine benefits the glucose homeostasis of juvenile blunt snout bream *Megalobrama amblycephala* fed a high-carbohydrate diet. *Aquaculture* **470**, 74–83.
31. Yu H, Zhang L, Chen P, *et al.* (2019) Dietary bile acids enhance growth, and alleviate hepatic fibrosis induced by a high starch diet via AKT/FOXO1 and cAMP/AMPK/SREBP1 pathway in micropterus salmoides. *Front Physiol* **10**, 1430.
32. Macfarlane S & Macfarlane GT (2003) Regulation of short-chain fatty acid production. *Proc Nutr Soc* **62**, 67–72.
33. Lynch KM, Lucid A, Arendt EK, *et al.* (2015) Genomics of *Weissella cibaria* with an examination of its metabolic traits. *Microbiology* **161**, 914–930.
34. Fidopiastis PM, Bezdek DJ, Horn MH, *et al.* (2006) Characterizing the resident, fermentative microbial consortium in the hindgut of the temperate-zone herbivorous fish, *Hermosilla azurea* (Teleostei: kyphosidae). *Mar Biol* **148**, 631–642.
35. Haenen D, Zhang J, da Silva CS, *et al.* (2013) A diet high in resistant starch modulates microbiota composition, SCFA concentrations, and gene expression in pig intestine1–3. *J Nutr* **143**, 274–283.
36. Venkataraman A, Sieber JR, Schmidt AW, *et al.* (2016) Variable responses of human microbiomes to dietary supplementation with resistant starch. *Microbiome* **4**, 33–33.
37. Agius L (2013) High-carbohydrate diets induce hepatic insulin resistance to protect the liver from substrate overload. *Biochem Pharmacol* **85**, 306–312.
38. Badman MK & Flier JS (2005) The gut and energy balance: visceral allies in the obesity wars. *Science* **307**, 1909–1914.
39. Murphy KG & Bloom SR (2006) Gut hormones and the regulation of energy homeostasis. *Nature* **444**, 854–859.
40. Mojsov S (2000) Glucagon-like peptide-1 (GLP-1) and the control of glucose metabolism in mammals and teleost fish. *American Zool* **40**, 246–258.
41. Wang Y, Dilidaxi D, Wu Y, *et al.* (2020) Composite probiotics alleviate type 2 diabetes by regulating intestinal microbiota and inducing GLP-1 secretion in db/db mice. *Biomed Pharmacother* **125**, 109914.
42. Ben-Shlomo S, Zvibel I, Shnell M, *et al.* (2011) Glucagon-like peptide-1 reduces hepatic lipogenesis via activation of AMP-activated protein kinase. *J Hepatol* **54**, 1214–1223.
43. Krieger JP, Langhans W & Lee SJ (2018) Novel role of GLP-1 receptor signaling in energy expenditure during chronic high fat diet feeding in rats. *Physiol Behav* **192**, 194–199.
44. Stone DAJ (2003) Dietary carbohydrate utilization by fish. *Rev Fisheries Sci* **11**, 337–369.
45. Hemre GI, Mommsen TP & Krogdahl Å (2002) Carbohydrates in fish nutrition: effects on growth, glucose metabolism and hepatic enzymes. *Aquacult Nutr* **8**, 175–194.
46. Gao Z, Wang X, Tan C, *et al.* (2019) Effect of dietary methionine levels on growth performance, amino acid metabolism and intestinal homeostasis in turbot (*Scophthalmus maximus* L.). *Aquaculture* **498**, 335–342.
47. Xu D, He G, Mai K, *et al.* (2016) Postprandial nutrient-sensing and metabolic responses after partial dietary fishmeal replacement by soyabean meal in turbot (*Scophthalmus maximus* L.). *Br J Nutr* **115**, 379–388.
48. Wang Q, He G, Mai K, *et al.* (2016) Chronic rapamycin treatment on the nutrient utilization and metabolism of juvenile turbot (*Psetta maxima*). *Sci Rep* **6**, 1–8.
49. Han SL, Wang J, Li LY, *et al.* (2020) The regulation of rapamycin on nutrient metabolism in Nile tilapia fed with high-energy diet. *Aquaculture* **520**, 734975.
50. Zhang H, Ding Q, Wang A, *et al.* (2020) Effects of dietary sodium acetate on food intake, weight gain, intestinal digestive enzyme activities, energy metabolism and gut microbiota in cultured fish: zebrafish as a model. *Aquaculture* **523**, 735188.
51. Li M, Hu F-C, Qiao F, *et al.* (2020) Sodium acetate alleviated high-carbohydrate induced intestinal inflammation by suppressing MAPK and NF-κB signaling pathways in Nile tilapia (*Oreochromis niloticus*). *Fish Shellfish Immunol* **98**, 758–765.

British Journal of Nutrition